Journal of
Marine Science and Engineering

MDPI

Article

Temporal (1948–2012) and Dynamic Evolution of the Wouri Estuary Coastline within the Gulf of Guinea

Yannick Fossi Fotsi [1,2,*], Nicolas Pouvreau [3], Isabelle Brenon [1], Raphael Onguene [2] and Jacques Etame [2]

1 Littoral, Environnement et Sociétés (LIENSs), UMR 7266 CNRS-Université de La Rochelle, 2 rue Olympe de Gouges, 17000 La Rochelle, France; isabelle.brenon@univ-lr.fr
2 Ufd bio-geosciences and environment, University of Douala, BP 24157 Douala, Cameroon; ziongra@yahoo.fr (R.O.); etame.jacques@yahoo.fr (J.E.)
3 Shom-French Hydrographic and Oceanographic Service, 29200 Brest, France; nicolas.pouvreau@shom.fr
* Correspondence: fossiyannick@gmail.com

Received: 23 August 2019; Accepted: 25 September 2019; Published: 30 September 2019

Abstract: The Wouri estuary is located in the Gulf of Guinea on the Atlantic coast of Cameroon's coastline plain (3°49′ and 4°04′ north latitude and 9°20′ to 9°40′ east longitude), and is strongly influenced by coastal dynamics that have remained unquantified over a long period of time. This study analyzed the historical evolution of the Wouri estuarine coastline between 1948 and 2012. Variations in the estuarine evolution of the Wouri were studied from (i) minute topographic extracts from 1948, (ii) 1996–1999 nautical charts, and (iii) 2012 spatial map vectors. The net temporal spatial variation rates were calculated using the statistical methods of the Digital Shoreline Analysis System (DSAS). These change rates were also calculated over two time intervals (1948–1996 and 1996–2012) and over a 64-year period (1948–2012). The study reveals highly disparate results. Indeed, kinematics show that the Wouri estuary was dominated by erosion in its downstream section, with 262.83 ha for −3.2 m/year and 110.56 ha for −5.8 m/year between 1948–1996 and 1996–2012 respectively, and by accretion on the other hand in its upstream section, with 239.17 ha for 4.3 m/year in zone 5 between 1948–1996 and 150.82 ha for 12.6 m/year in zone 4 between 1996–2012. Thus, over the 64-year period (1948–2012), we have a dominance of variation by erosion downstream and conversely by accretion upstream, marked by the presence of amplifying factors (anthropogenic pressure and climate change) of the rate of variation of morphological evolution at the beginning of the 21st century, as compared to the middle-20th century. The observed development of sediment loss and accumulation, both influences and will influence, the sediment regime along the Wouri estuarine coastline. There is a need to develop a systematic sub-regional coastal surveillance activity to effectively manage Cameroon's coastline system.

Keywords: shoreline change; erosion; accretion; Wouri estuary; climate change

1. Introduction

In recent years, shoreline position changes have become one of the major environmental problems affecting coastal zones worldwide. Indeed, 24% [1] to 70% [2] of the world's sandy beaches are estimated to be under erosion. The West African coasts, largely composed of estuaries and beaches, are no exception to this trend. According to the authors of [3], retreat in the sandy coastline in the Gulf of Guinea between Côte d'Ivoire and Cameroon is very significant, with rates of around 1 to 5 or even 10 m/year. This situation has remained very worrying since the construction of marine works in the 1960s and due to the importance of human interventions on the coastal fringe [4,5], not to mention the impact of climate change [6,7]. This is the case of the Wouri estuary, left in its natural state until

the beginning of 1940, which has been the subject of major regional development in recent decades. This development was marked by the extension and modernization of the Douala Autonomous Port, the creation of industrial areas for railways and infrastructures [8]. These development operations have contributed to the economic development of this environment, but they have also destabilized the natural balance of this coastal area, which now supports a high density of infrastructure. Also, being open to the Atlantic Ocean, the Wouri estuary is subject to marine turmoil, and as a result, has experienced significant variations in the coastline, with a retreat of about 3 m per year, at the risk of losing a mangrove island to the sea (89%) [9]. This has forced hundreds of people to abandon their homes [10].

In this context, studies by the authors of [11–13] have addressed the spatial and temporal evolution of the degradation of the vegetation cover of extracts from the Wouri estuarine coastline (Cameroon) in the face of climate change, in order to estimate the retreat rates of the coastline and assess their vulnerability. The authors of [14] conducted a study on the assessment of the Cameroonian coastline to understand the general trend of coastal evolution and showed the significant areas of change (accretion/erosion) observed in an extract from the Wouri estuary. The authors' research was based on a series of Landsat images taken between 1975 and 2016. The results of such studies contribute to the development of coastal management policies and promote the development of sustainable management practices in the coastal regions of developed countries. However, in Africa and particularly in Cameroon, no study has yet been the subject of a sustainable coastal zone management response, due to the fundamental lack of reliable historical coastal data available. Studies that have already carried out on the coastal zone of Cameroon have used Landsat image series, available only since 1972. The Wouri estuary, a coastline area of high economic interest in Cameroon since the urban and tourism boom, with accelerated population growth (5% per year) [15], has not yet been the subject of a full study of the evolution of its coastal area. So, in response to the development challenges for better and sustainable management of the estuary coastline of Wouri in Cameroon, a study such as ours is both urgent and necessary.

In this study, we use ancient archives (topographic minutes), marine charts and spatial map vectors, to analyze the evolution of the Wouri estuarine coast over a period of 64 years. We use geospatial techniques, a geographic information system (GIS) and analysis of several statistical approaches to add to the DSAS model [16]. For analysis, several statistical approaches have been used to determine the rates of shoreline changes, including end point rate (EPR), linear regression rate (LRR) and weighted linear regression rates (WLR) [17–20]. The main objective of this work is to map and quantify the erosion and accretion areas and to evaluate the long-term rates of changes along the Wouri estuarine coastline (Cameroon).

2. Study Area

The hypo-synchronous Wouri estuary [21,22] covers an area of 1200 km^2 and is a vast wetland 30 km long and almost as wide, open to the Atlantic Ocean [23]. Located at 4°0′1″ north latitude and 9°37′15″ east longitude, it occupies the heart of the Douala sedimentary basin (19,000 km^2 of which 7000 km^2 emerged), centered on an old syncline with pan-African mylonites, and the axis of this is where the lower Wouri flows [24]. The estuary is home to the Autonomous Port of Douala (PAD), the largest port in the country and one of the most important in Central Africa. Bound to the north by Douala and to the south by Souellaba, this geographical area is drained by three coastal rivers: the Dibamba, the Wouri and the Mungo (Figure 1). It enjoys an equatorial coastal climate with two dry seasons from October to May interspersed with two rainy seasons. The region receives 3.5 to 4.5 m of precipitation per year, with an average temperature of 26.4 °C. The air is almost constantly saturated (99% in the rainy season and 80% in the dry season). Tropical cyclones are unknown despite the strong influence of tides, of the semi-diurnal type, with an average amplitude of 2.5 m [25]. In this environment, altitude differences remain low, reliefs rarely exceed three meters, and there are residues of sandy cords, small sandy islands and mio-pliocene gravels, sometimes bearing an iron armor.

The vegetation is a mangrove composed of Rhizophoras up to 40 m high and avicennias that colonize the intertidal spaces of the fine sedimentation grounds [9,26,27]. All parts of the estuary that are subject to fine sedimentation from fluvial origin have dense and extensive mangroves. The sedimentation and erosion pattern is determined by hydrological and geomorphological factors that show diurnal and seasonal variations under the influence of tides, currents and freshwater flows [24].

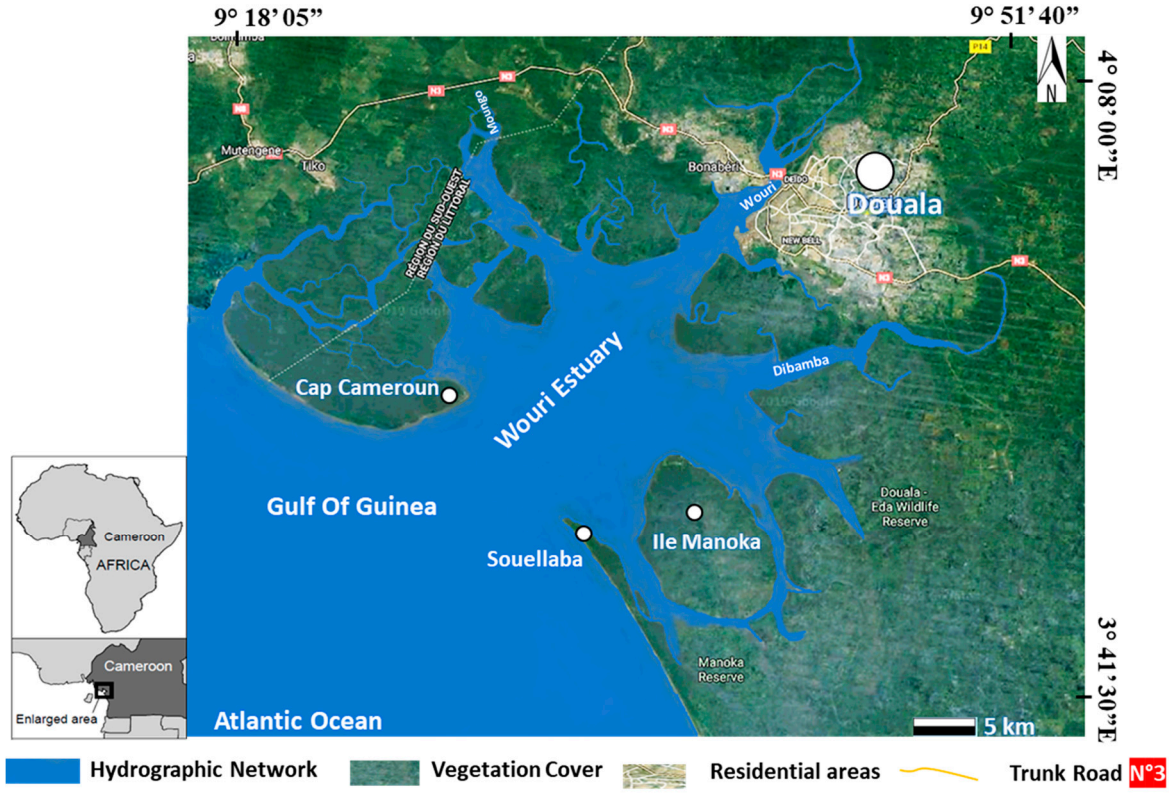

Figure 1. Estuary Wouri in the Atlantic coastal Cameroon.

3. Materials and Methods

3.1. Data Sources

In this study, the data sources used to detect shoreline changes in the Wouri estuary are the following:

Topographic surveys of the Shom archives (French Hydrographic and Oceanographic Service) of the Wouri estuary from 1948 (or 1949/1950) to the present date, of various spatial scale, were georeferenced, then given geometric correction with Scanbathy software [28], mosaicked into one, and saved as an uncompressed TIFF using WGS84/32 North in UTM (Figure 2A and Table 1). The planimetric accuracy of 16 m was quantified by comparing the locations of the reference points (6 points) on the historical map with their true locations, using the current image provided by the Google Earth program, projected in UTM 32 north on WGS84 (Figure 2A and Table 1). These topographic surveys are obtained by the triangulation method targeting landmarks (e.g., lighthouses, churches, temples, bridges). Hydrographic engineers identify the land landmarks for which they calculate the distances and angles between them. Once at sea, at least three of these landmarks are used to precisely locate the contours of the coast on a map. The authors of [29] explain that engineers "draw by show of hands, according to the method of identifying between the sufficiently close milestones on this subject facing the resulting dangers." Upgrading problems are reduced to their simple expression [30].

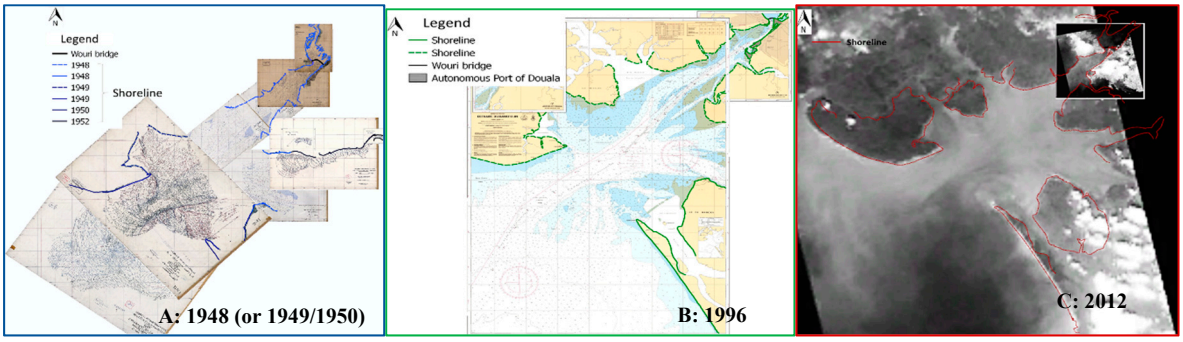

Figure 2. Presentation of extracting data sources in the coastline between 1948 (or 1949, 1950) to 2012.

Table 1. Characteristics data.

Date	1948 or (1949, 1950)	1996 (1999)	2012
Data	Topographic surveys	Nautical chart surveys N°7578	Digital topographic space map S201201300
Scale	1/10,000 (1948) 1/15,000 (1949) 1/25,000 (1950)	1/40,000	-
Type	Raster (Geo Tiff)	Raster (Geo Tiff)	Vector

Nautical chart surveys N°7578, from the archives of the Shom [31] describing the coastline from the interpretation of SPOT satellite data (CNEC, National Environmental Monitoring Centre 1996) and ERS-1 and ERS-2 satellites (1994–1999) after treatment (Figure 2B and Table 1) (ERS, European Remote Sensing satellite system). Regarding the precision of the calculations between the two georeferences (SPOT and ERS), as per [32], the results on the city of Douala, it can be seen that the concordance of the coordinates is satisfying (10 m of X and 30 m Y deviations) compared to the system resolutions (respectively 25 and 20 m for ERS and SPOT). However, there is a systematic deviation along the Y axis of 35 m. Conversely, after comparing the positions of the reference points (6 points) on the nautical chart with their true positions using the current image provided by the Google Earth program, projected in UTM 32 north on WGS84, the planimetric accuracy is 27 m. In short, the planimetric accuracy of these images is guaranteed at 35 m.

A digital topographic space map S201201300 of the Wouri estuary and Bioko Island (Africa) is created, from panchromatic optical and radar imagery, multispectral images, photographs, books on spatio-preparation, marine charts, lifting doubts and Google Earth after treatment (Figure 2C and Table 1). According to the authors of [33], this map is geo-referenced in the equatorial Mercator projection on WGS84 and has an absolute planimetric accuracy of less than 20 m. This is readable in all geographical information systems.

3.2. Shoreline Extraction and Error Evaluation

In this study, the most common detection technique applied to visible reference lines (shorelines) on documents (2A and 2B) made by surveyors or hydrographers during its preparation was used and the shorelines were digitized. For the digital topographic space map S201201300, the shorelines were derived from clearly visible coastal elements (using true or false color images) and by the application of digital processing techniques (geometric and radiometric) of images and photo-interpretation [33]. After obtaining digital shoreline data, they were compiled in a GIS environment (Arcgis 10.5 software) and analyzed by the Digital Coastal Analysis System (DSAS) developed by the United States Geological Survey (USGS).

Before any analysis, the evaluation of errors in relation to each shoreline position is required and must be calculated before drawing conclusions on the evolution of the shoreline [33]. Indeed, since

data sources are second-hand and from satellites, they include sources of uncertainty related to the quality of the data used (pixel error (Ep)), geo-referenced images (RMSE (ERMs)), coastal extraction and digitization (digitization error (Ed)) and planimetric uncertainty (EP). These errors are considered random and uncorrelated, the total of the errors (Et) is given by the square root of the sum of the squares of the different variables (Equation (1)) [18,34]:

$$\boldsymbol{Et} = \pm\sqrt{Ep^2 + ERMs^2 + Ed^2 + EP^2} \quad (1)$$

The total error was estimated from two sources (Table 2): (1) the total shoreline position error was calculated for three dates; (2) the measured (Em) and annualized (Ea) transect error associated with the rate of shoreline change at a given transect. It was calculated over two short time periods: (1948–1996, 1996–2012) and over a global period (1948–2012). The annualized error was calculated using the following Equation (2):

$$\mathbf{Ea} = \frac{\sqrt{Et1^2 + Et2^2 + Et3^2}}{\text{Total period (Years)}} \quad (2)$$

Table 2. Summary of errors and estimation for periods of study.

Date	1948 or (1949, 1950)	1996 (1999)	2012
Error pixel (Ep)	1	4	/
RMS ortho-rectification (ERMs)	16	27	/
Digitizing error (Ed)	5	11	/
Planimetric Error (EP)	/	35	21
Total error (Et)	17	46	21
Year	1948–1996	1996–2012	1948–2012
Measured Error (Em) (m)	49	51	27
Annualized Error (Ea) (m/64 years)		0.83	
The uncertainty of end point rate calculation (ECI) (m/year)	1	3.2	0.42

The annualized uncertainty over a time period of 64 years is therefore 0.68 m/year (Table 1). Recently, the uncertainty associated with the computation of the end point rate (EPR) is automatically calculated in the application of DSAS. The result of this computation is specified as confidence of the end point rate calculation (ECI) [16]. The ECI is calculated using Equation (3):

$$\mathbf{ECI} = \frac{\sqrt{EtA^2 + EtB^2}}{\text{date (A)} - \textit{date (B)}} \quad (3)$$

where (EtA) is the uncertainty of the position of shoreline A, (EtB) is the uncertainty of the position of shoreline B, date (A) is the date of shoreline A and date (B) is the date of shoreline B.

Again, the error (ECI) is calculated on two short periods of time (Table 1): 1948–1996, 1996–2012, and on a global period (1948–2012).

3.3. Analysis of Coastal Variations

The model DSAS (5.0) developed by the USGS [16] was used to estimate the shoreline change rates of the Wouri estuary. The DSAS is based on the measurement of the basic method used for calculating change rate statistics for a time series of shores and carried out in four steps: (1) shoreline and (2) baseline digitization, (3) generation of transects, and (4) computing the shoreline change rate.

The 1948 (or 1949, 1950) and 2012 coastlines were stored in a geodatabase with the WGS 84/UTM zone 32N coordinate system. The baseline, constructed to serve as a starting point for all transects derived by the DSAS application, was created either offshore or onshore and parallel to the general trend of the shorelines. Intersections of shore transecting along the baseline were then used to calculate the rate of change statistics [35]. Based on the DSAS parameters, about 8400 transects were generated every 10 m, perpendicular to the baseline.

In this study, the net shoreline movement (NSM), end point rate (EPR), linear rate regression (LRR) and weighted linear regression (WLR) were used for calculating the rate of change of the coastline. The NSM reports the distance between the oldest and the youngest shorelines. The EPR was calculated by dividing the distance (in meters) separating two shorelines (NSM) by the number of years between the dates of the two shorelines, in Equation (4):

$$\mathbf{EPR} = \frac{\mathbf{D1} - \mathbf{D2}}{\mathbf{t1} - \mathbf{t0}} \quad (4)$$

where: **D1** and **D2** represent the distance separating the shoreline and baseline, and **t0** and **t1** are the dates of the two shoreline positions.

The second method used for calculating erosion rates is through LRR. This method consists of fitting a least square regression line to multiple shoreline position points for a particular transect. The shoreline change rate along each transect for all periods (1948–2012) was computed by plotting the points where shorelines are intersected by transects and calculating the linear regression equation, which has the form: y = a + bX, where, (y) represents the distance, in meters, from the baseline (1948), (X) shoreline dates (years), (b) represents the shoreline change rate and (a) is the y-intercept.

In this study, the R-squared, $R^2 > 0.8$ has been retained as the limit of certainty. The uncertainty of the reported rate is considered with a confidence interval (LCI) of 95%. In contrast, with the WLR, more reliable data are given greater emphasis or weight towards determining a best-fit line with a confidence interval of 99.9% [19]. The WLR rate is determined by plotting the shoreline positions with respect to time. The weight (**w**) is defined as a function of the variance in the uncertainty of the measurement (**e**) [16], as in Equation (5):

$$\mathbf{w} = 1/\mathbf{e}^2 \quad (5)$$

Considering the overall error (Table 2), changes in Wouri estuarine shoreline are shown in Table 3 with NSM (m) and EPR, LRR, WLR (m/year) and for a detailed analysis following the methodical flowchart summarized in Figure 3, the Wouri Estuary was subdivided into 8 zones (see Figure 4).

Table 3. Variation of the estuarine Wouri shoreline.

Periods	Change Shoreline	Erosion	Stable	Accretion
1948–1996	m	<-49	±49	>49
	m/year	<-1	±1	>1
1996–2012	m	<-51	±51	>51
	m/year	<-3.2	±3.2	>3.2
1948–2012	m	<-27	±27	>27
	m/year	<-0.42	±0.42	>0.42

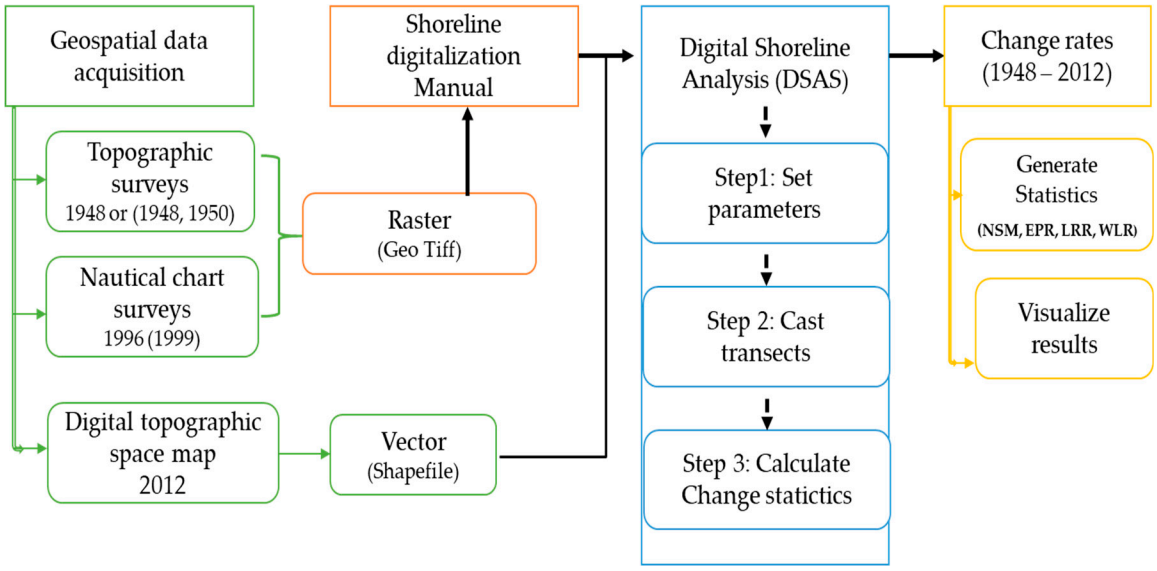

Figure 3. Methodology flowchart.

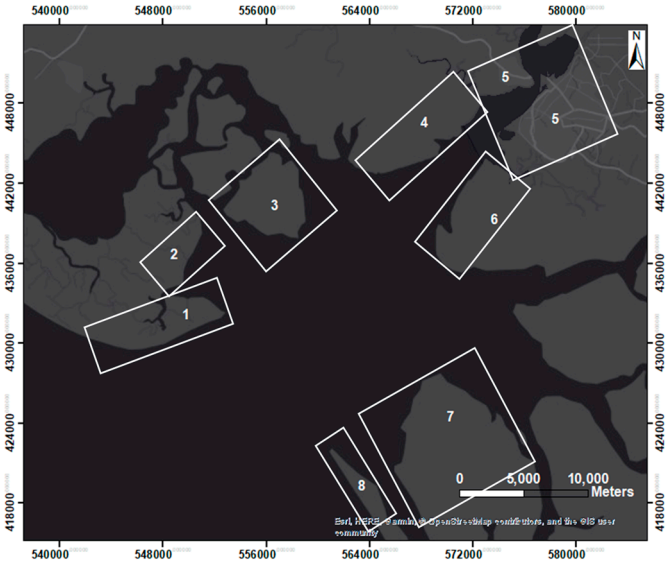

Figure 4. Subdivision of the Wouri estuary into 8 zones.

4. Results

4.1. Shoreline Kinematic of Wouri Estuary between 1948–2012

The superposition of the 1948–2012 coastlines (Figure 5) shows a variability in spatial evolution over time, from the upstream (Douala) to downstream (Cape Cameroon, Souellaba). This variability presents the amplitudes of the observed time lags and is defined as the difference between the position of the rearmost line on the land side, and the most advanced one in the sea. Using the DSAS model, we quantify and qualify the kinematics of the Wouri estuary coastline.

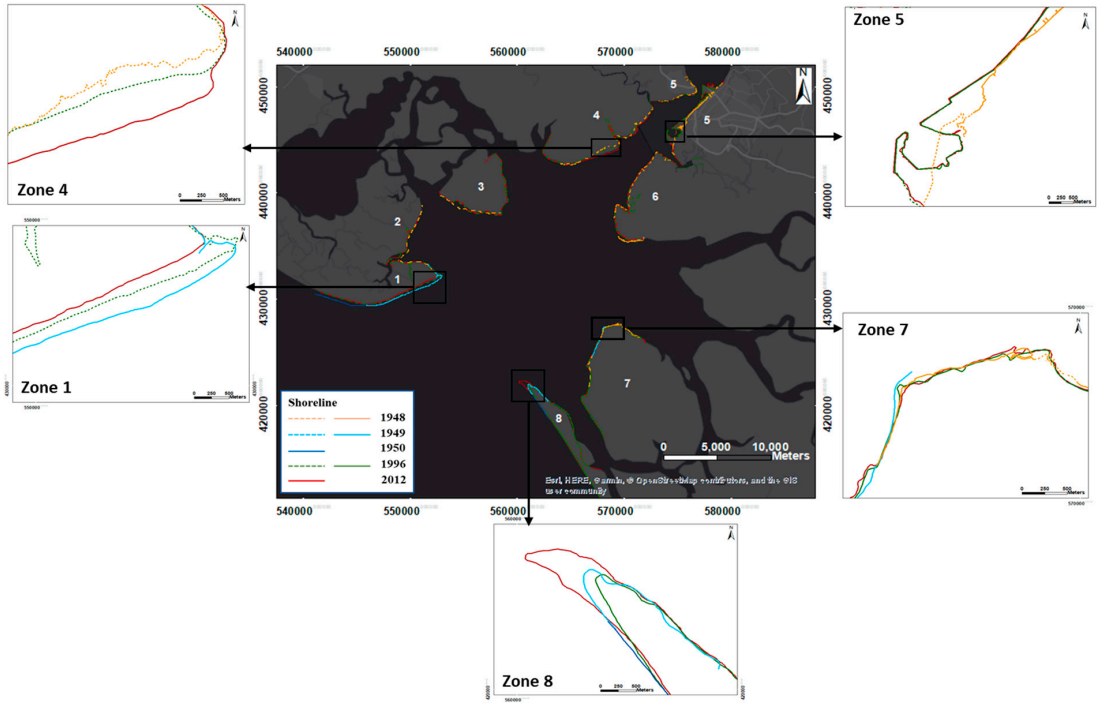

Figure 5. Shoreline kinematics of the Wouri estuary between 1948 (or 1949, 1950) and 2012.

4.2. Shoreline Changes in the Wouri Estuary

The analysis of the shoreline evolution of the Wouri estuary from 1948 (or 1949, 1950) and 2012 shows that over time and zones, the estuarine coastal Wouri has changed significantly (Figure 4). These variations are expressed by erosion and accretion. A thorough analysis of changes using the EPR, LRR, LWR and NSM methods have allowed for the construction of spatiotemporal maps, histograms and tables.

4.2.1. Period 1948–1996

The statistical results obtained during this period of time (48 years) on the whole study area show that the shoreline oscillates between retreat–stability–advanced and retreat–stability. Along the Wouri estuarine coastline, 29.13 km or 35% of transects are eroded, while 19.36 km or 23% of transects increase, and 35.06 km or 42% of transects remained stable (Figure 6 and Table 4). In detail, zone 1 shows a large dominance of variation by erosion, with an average erosion rate of −3.2 m/year and zone 5 shows a large dominance of variation by accretion with an average accretion rate of 4.3 m/year (EPR) (Figure 6a). Also, the NSM method (Figure 5b and Table 4) emphasizes that the maximum eroded transect distance of 518 m with a rate of evolution of 12.06 m/year is observed in zone 3 and conversely the maximum accumulated transect distance of 1089 m with a rate of 23.71 m/year is observed in zone 5. The significant accumulation observed in zone 5 is due to the backfill for the expansion of the PAD for reasons of economic development, which began in the early 1980s.

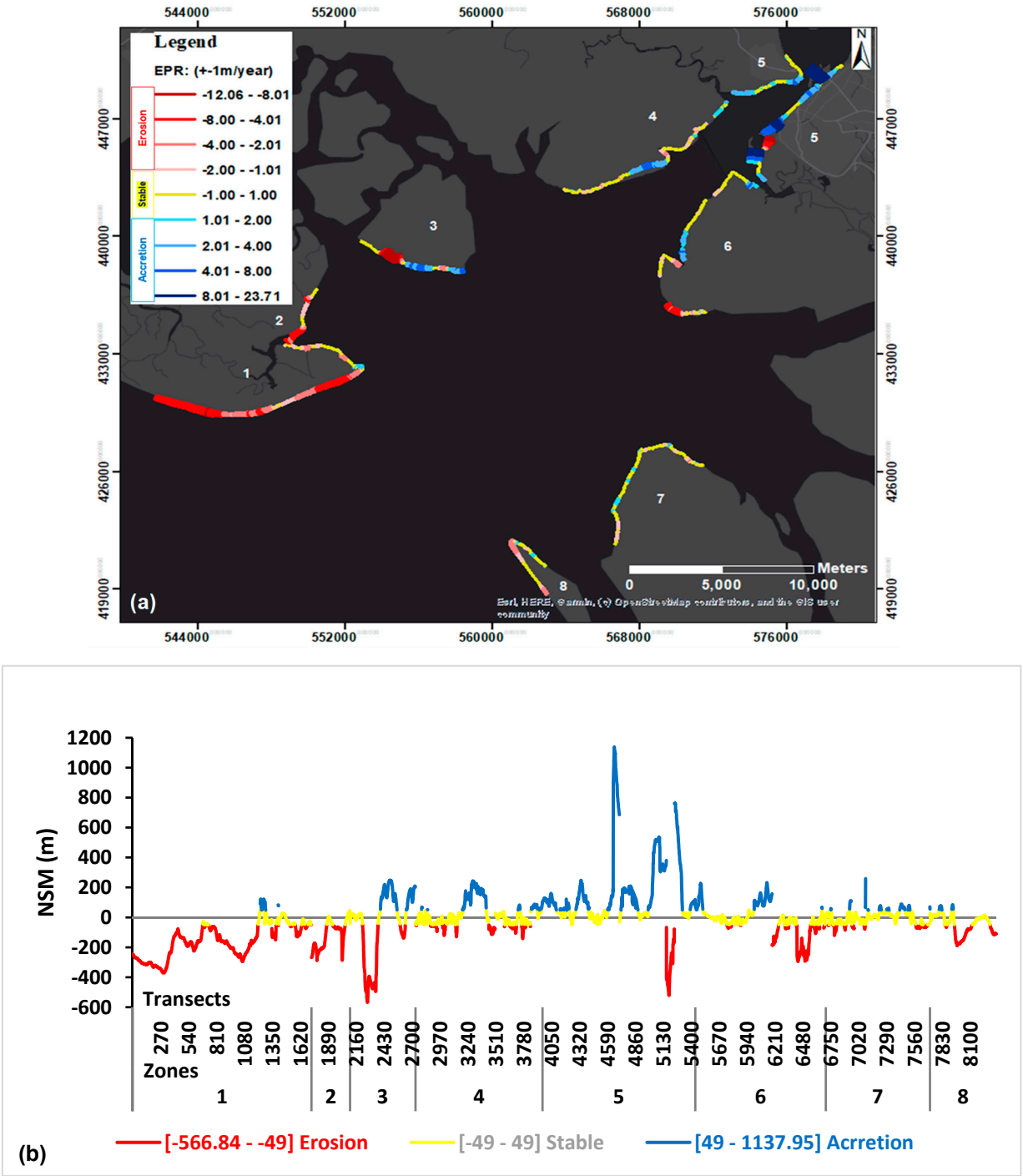

Figure 6. Shoreline evolution between 1948 and 1996 in the Wouri estuary, (erosion and accretion) computed by the end point rate (EPR) (**a**), and net shoreline movement (NSM) (**b**) methods.

Table 4. Statistical data of the study area during 1948–1996.

Shoreline Classification	Shoreline Statistics		Zones							
			1	2	3	4	5	6	7	8
Erosion	EPR	Mean	-3.2	-2.2	-5.8	-0.6	-5.8	-2.0	-0.4	-1.4
	NSM	Min	-321.5	-238.8	-517.8	-92.5	-471.9	-245.1	-71.4	-139.7
	Transects		1352	272	203	240	77	328	185	256
Accretion	EPR	Mean	0.8		2.4	1.7	4.3	1.5	0.5	0.5
	NSM	Max	74.0		199.7	195.1	1089.0	182.9	209.2	35.8
	Transects		51	0	250	330	872	250	139	44
Stable	Transects		327	101	180	659	529	685	683	342

4.2.2. Period 1996–2012

During this period, the estuarine coastline of Wouri Cameroon oscillates between stability–retreat–advanced and stability-advanced. Essentially, this period is marked by a dominance of no variation of the coastline, with 86.45 km or 79% of the transects analyzed being stable, versus 11.26 km or 10% of transects being eroded, and 12.21 km or 11% of transects being in accretion. As in the previous period, zone 1 shows a large dominance of variation by erosion with an average erosion rate of −5.8 m/year, unlike the dominance of variation by accretion with an average accretion rate of 12.6 m/year observed here in zone 4 (Figure 7a). The NSM method (Figure 7b and Table 5) points out that the maximum eroded transect distance of 428 m, with a change rate of 31.92 m/year, is observed in zone 1 and the maximum cumulative transect distance of 996 m with a rate of 69.35 m/year is observed in zone 8. In detail, different from the observations of the previous period, we observe during this period an important evolution of the accretion in zone 4, and the absence of variation observed in zone 5, due to the construction of the dike of the PAD. Furthermore, in zone 8, we also observe an inversion of the tendency of variation of the erosion for the accretion.

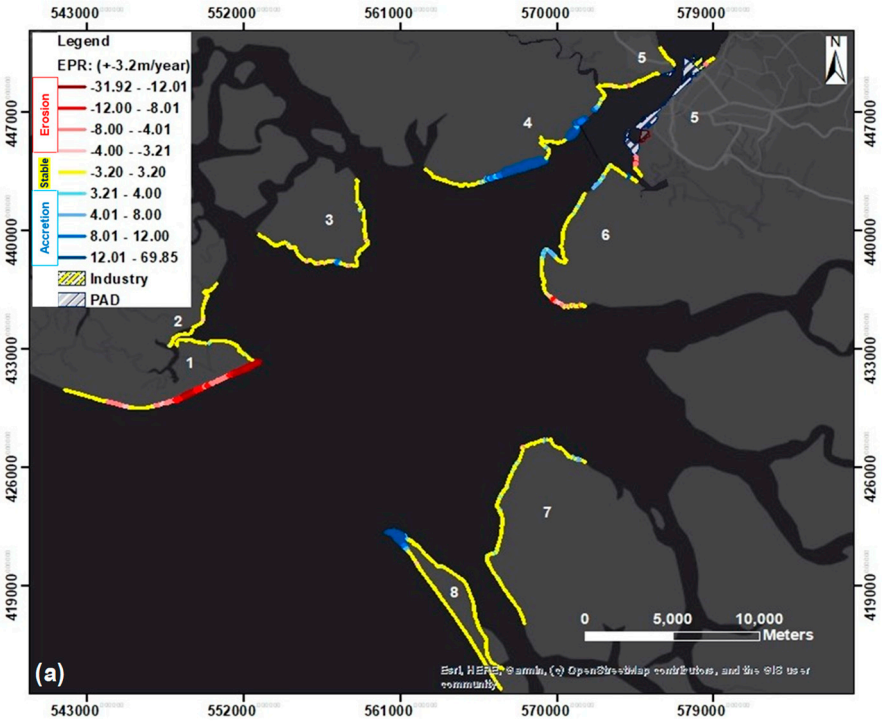

Figure 7. *Cont.*

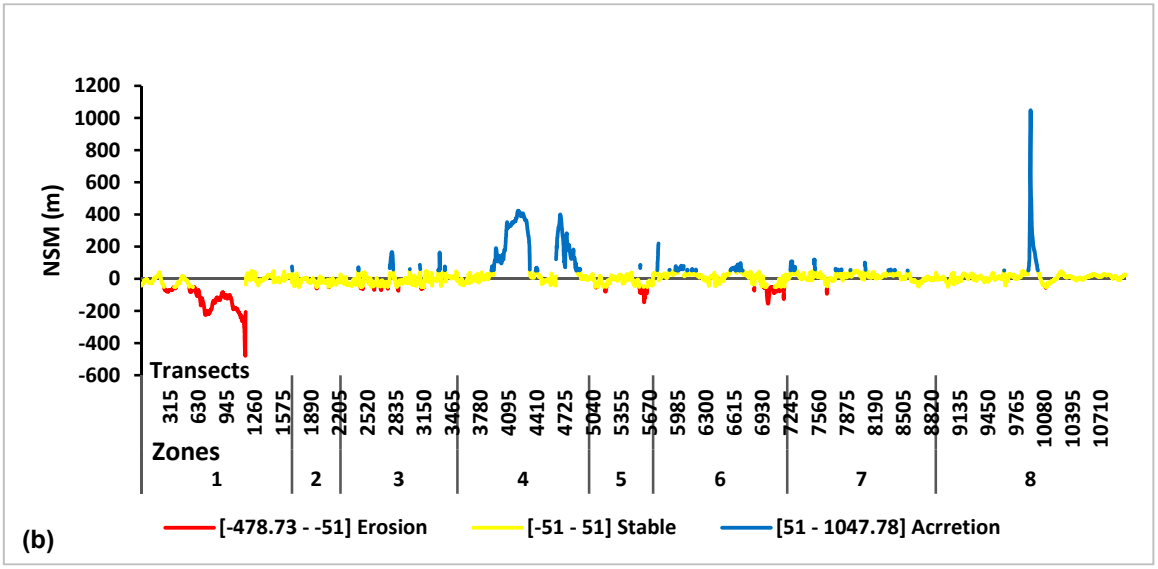

Figure 7. Shoreline evolution between 1996 and 2012 in the Wouri estuary, (erosion and accretion) computed by the EPR (**a**), NSM (**b**) methods.

Table 5. Statistical of the study area during 1996–2012.

			Zones							
Shoreline Classification	**Shoreline Statistics**		**1**	**2**	**3**	**4**	**5**	**6**	**7**	**8**
Erosion	EPR	Mean	-5.8	-0.4	-0.7	-3.2	-1.8	-1.8	-2.0	-0.2
	NSM	Min	-427.7	-9.2	-23.4	-51.0	-95.3	-103.4	-42.4	-4.3
	Transects		760	18	72	0	108	151	8	9
Accretion	EPR	Mean	0.2	1.1	3.2	12.6	2.1	1.2	1.3	12.1
	NSM	Max	1.5	25.7	115.3	371.9	35.5	168.9	68.9	996.8
	Transects		2	4	78	687	3	235	102	110
Stable	Transects		920	520	1155	784	604	1113	1549	2000

4.2.3. Period 1948–2012

During the overall period 1948–2012 (64 years), the results show a coastline position that varies between retreat and advanced, in proportion to 37.4% and 39.4% of transects analyzed respectively. Zone 1 (Cape Cameroon) at the mouth of the estuary is largely dominated by erosion with an average rate of change of −3.8, −3.7, −3.8 m/year (EPR, LRR, WLR). Zones 4 and 5 (Douala) upstream of the estuary are dominated by accretion, with average changes rates of 3.9, 3.3, 3.7 and 3.4, 3.4, 3.3 m/year (EPR, LRR, WLR) respectively (Figure 8 and Table 6). The maximum eroded distance (−552 m) with a rate of change of −8.71 m/year is recorded in zone 3, and conversely, 1115 m (14.16 m/year) of the maximum advanced distance recorded in zone 5. The coastline in the Wouri estuary reveals that over the past 64 years, 37.24 km of the coast has been eroded, compared 32.91 km that has been in accretion and the remaining 19.42 km has shown no variation.

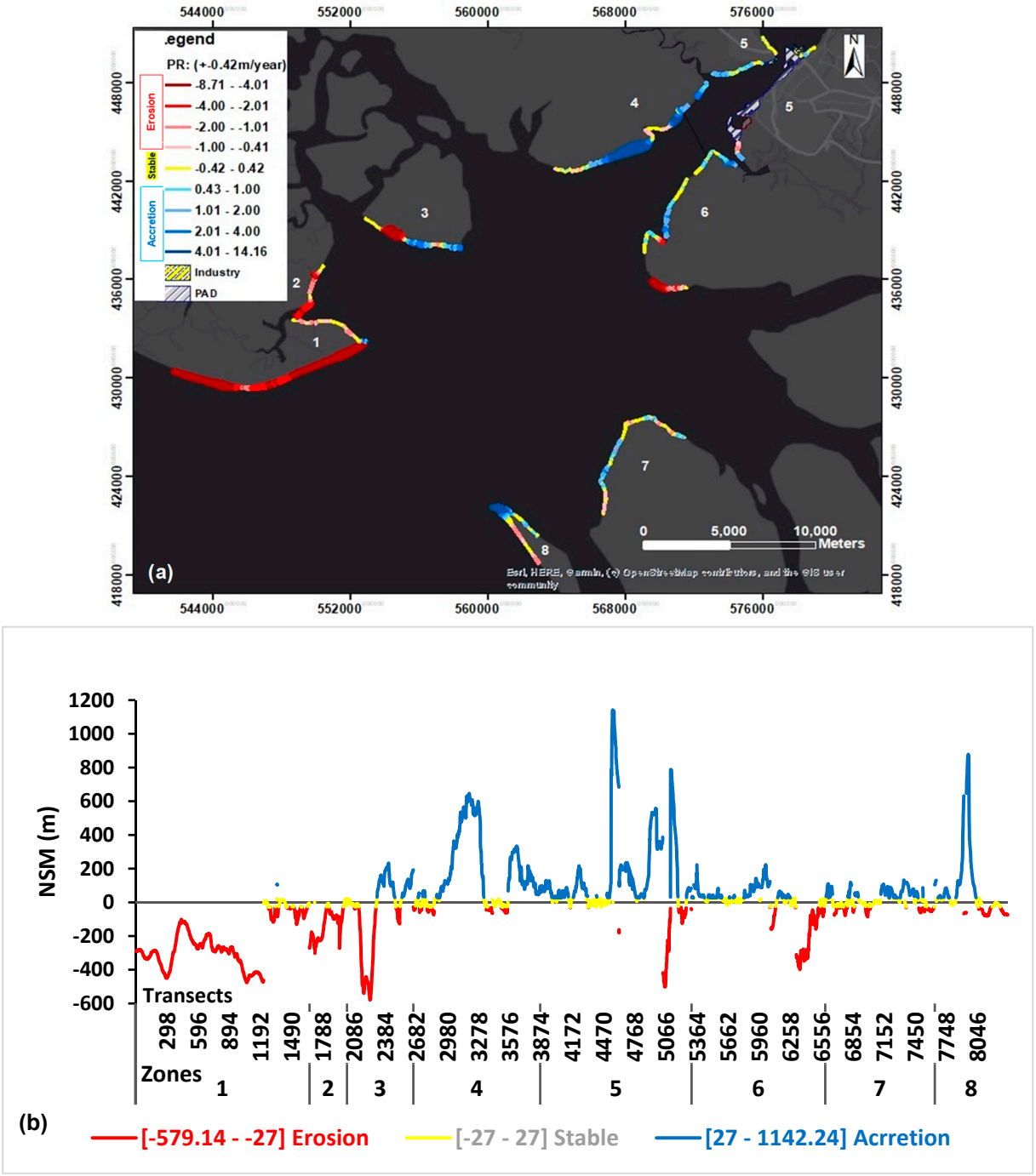

Figure 8. Shoreline evolution between 1948 and 2012 in the Wouri estuary, (erosion and accretion) computed by the EPR (**a**), NSM (**b**) methods.

Table 6. Total statistics of the study area during 1948–2012.

	Zones							
	1	**2**	**3**	**4**	**5**	**6**	**7**	**8**
Shoreline length that recorded erosion (NSM (m))								
Min	-448.7	-275.2	-552.1	-46.9	-474.5	-371.3	-58.3	-54.5
Shoreline length that recorded accretion (NSM (m))								
Max	79.8	0	205.9	619.1	1115.2	196.6	105.5	850.9
Mean rate erosion (m/year)								
EPR	-3.8	-2	-4.4	-0.3	-2.6	-2.6	-0.3	-0.5
LRR	-3.7	-2.1	-4.6	-0.4	-3	-2.5	-0.4	-0.6
WLR	-3.8	-2	-4.5	-0.3	-2.7	-2.6	-0.4	-0.6
Mean rate accretion (m/year)								
EPR	1.3	-	1.5	3.9	3.4	0.7	0.8	2.7
LRR	1.2	-	1.9	3.3	3.4	0.9	0.7	2
WLR	1.3	-	1.6	3.7	3.3	0.7	0.7	2.5
Total transects that recorded erosion								
EPR	1482	300	219	191	163	303	253	213
LRR	1507	297	225	212	137	307	313	252
WLR	1488	300	217	206	154	300	292	209
Total transects that recorded accretion								
EPR	7	0	297	775	945	584	422	261
LRR	6	2	265	737	971	428	373	221
WLR	6	0	276	755	944	507	404	247
Total transects that recorded as stable								
EPR	174	59	136	247	339	391	372	224
LRR	150	60	144	264	339	543	361	225
WLR	169	59	141	252	349	471	351	242
% of total transects that recorded erosion								
EPR	47.4	9.6	7.0	6.1	5.2	9.7	8.1	6.8
LRR	46.4	9.1	6.9	6.5	4.2	9.4	9.6	7.8
WLR	47.0	9.5	6.9	6.5	4.9	9.5	9.2	6.6
% of total transects that recorded accretion								
EPR	0.2	0.0	9.0	23.5	28.7	17.7	12.8	7.9
LRR	0.2	0.1	8.8	24.5	32.3	14.3	12.4	7.4
WLR	0.2	0.0	8.8	24.1	30.1	16.2	12.9	7.9
% of total transects that recorded as stable								
EPR	9.0	3.0	7.0	12.7	17.5	20.1	19.2	11.5
LRR	7.2	2.9	6.9	12.7	16.3	26.0	17.3	10.8
WLR	8.3	2.9	6.9	12.4	17.2	23.2	17.3	11.9

4.3. Surface Balance Sheets of Study Area Beaches and Total Coastal Sediment Budget

The measurement of linear changes in the Wouri estuarine shoreline, complemented by surface sediment budgets calculation, offers a vision of the coastal kinematics in two dimensions. In this regard, surface sediment budgets for all study areas in the Wouri estuary for each period have been recorded and are presented in Figure 9. The following results show spatial and temporal variability along the coastline. According to these results, the areas of lost areas (113.3 ha) dominate by −0.5 ha those obtained by accretion (112.3 ha), and the overall sediment budget of 64 years is negative. Zone 1, which is largely dominated by erosion, has a sediment loss of about 378.8 ha (−5.92 ha/year) and conversely, zones 4 and 5 have gains of 183 m (2.86 ha/year) and 212.3 (3.32 ha/year) respectively between 1948–2012.

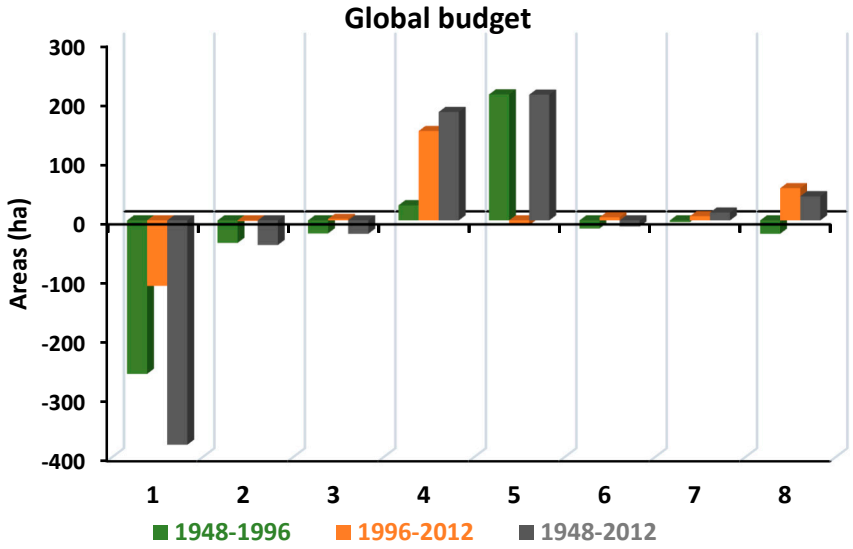

Figure 9. Sedimentary budget along the coastline of the Wouri estuary for each period.

During these two periods, 1948–1996 and 1996–2012, studied, losses were largely recorded in zone 1, with 110.4 ha of land lost in 16 years, versus 259 ha in 48 years. Conversely, zones 5 and 4 recorded strong gains in sedimentary surface area. Between 1948 and 1996, a total of 212.66 ha of surface gains were recorded in zone 5, due to the embankments for the expansion of the PAD. Between 1996–2012, a total of 150.92 ha of surface gains were recorded in zone 4. Also, in zone 8, we recorded a reversal of the trend between the two periods as we moved from an erosion zone (−22.6 ha lost between 1948–1996) to an accretion zone (54.42 ha gained between 1996–2012).

5. Discussion

The global evolution of the Wouri estuarine coast, between 1948 and 2012, shows a slightly positive evolution rate because it is subject to accretion (39%), erosion (37%) and stability (23%). The evolution rates, obtained by three statistical approaches (EPR, LRR and WLR), are very similar throughout the study zones (Figure 10 and Table 6). After comparing the EPR vs. LRR, EPR vs. WLR values, the R-squared values obtained between 1948 and 2012 indicate a very good correlation between the dependent and independent variables (Figure 10a,b). This correlation results obtained in studies on the change of the sandy coast are similar to those of [19,36,37].

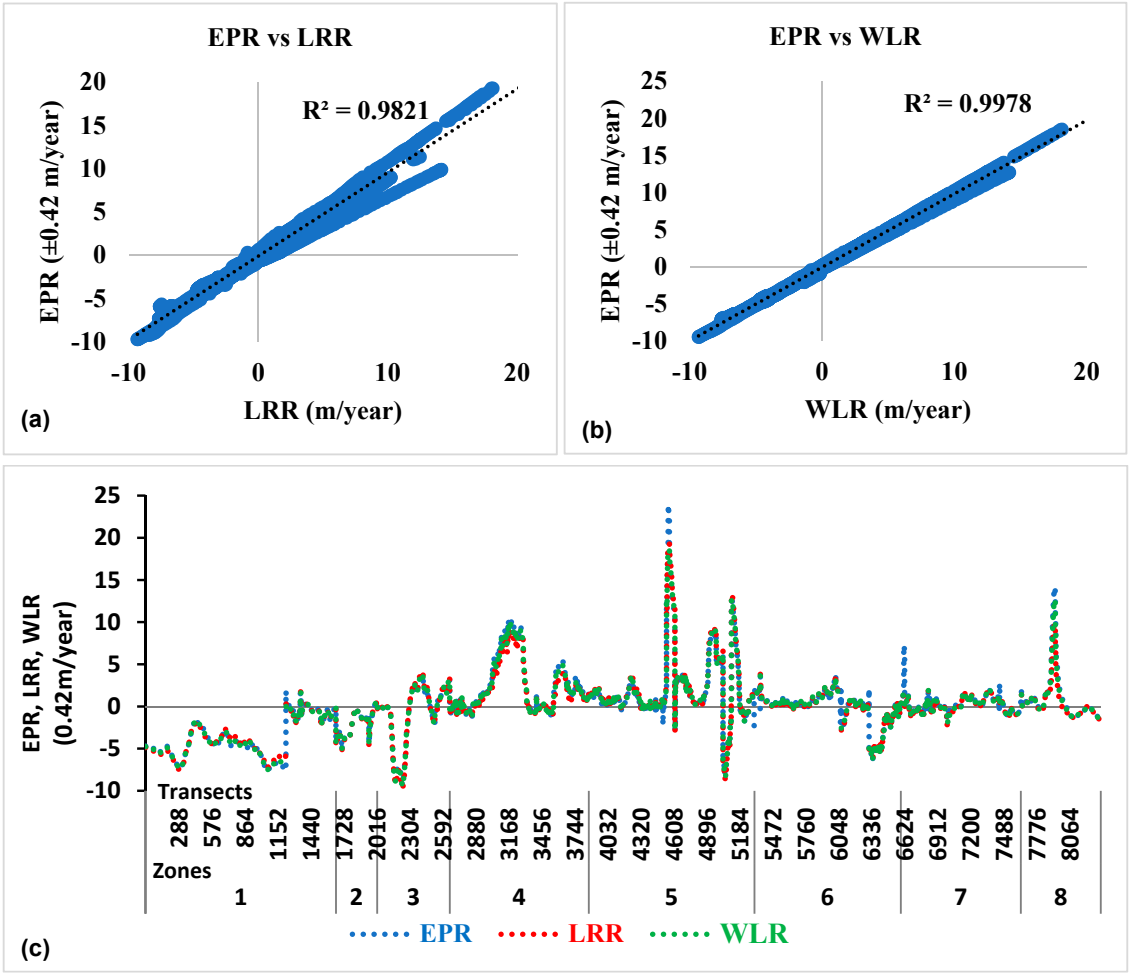

Figure 10. (**a**,**b**) Comparison of shoreline rates obtained by different statistical methods (EPR, linear regression rate (LRR) and weighted linear regression rates (WLR)) for all transects of the study area. (**c**) The EPR, LRR and WLR values (m/year) calculated along all transects (8340) and zones (8) of the study area during the whole period (1948–2012).

In detail, this study notes that, on the one hand, between the period 1948–1996, 35% or 29.13 km of the area studied demonstrates erosion, strongly represented in the downstream section of the estuary (zone 1). Additionally, in 23% or 35 km of the area studied, accretion is strongly represented in the upstream of the estuary in zone 5, versus 42% or 35.06 km of stability, which is strongly represented in zones 6 and 7. On the other hand, during the period 1996–2012, 10% or 11.26 km of the eroding surface is still strongly represented in the lower section of the estuary (zone 1) and 11% or 12.21 km of accretion is strongly represented in zone 4, versus 79% or 86.45 km of stability, which is strongly represented in zone 8. Wouri estuary shoreline changes, based on these periodic subdivisions, are controlled by natural processes, human activities and climate change (Figures 11–15).

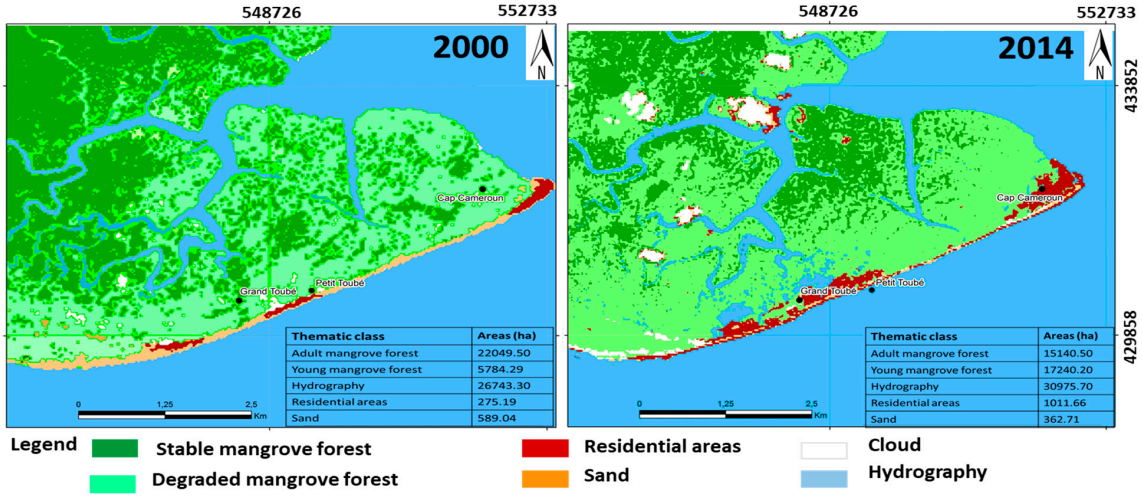

Figure 11. Illustration of the changes that have affected zone 1 between **2000–2014**, that are responsible for its geomorphological evolutions

Figure 12. Illustration of the rising waters, with the immersion of the communication relay antenna in the sea, installed off the mainland of Cap Cameroun around 1993 (adapted from the study of Tchindjang et al. [38] based on vulnerability and adaptation of Cap Cameroun populations to natural risks).

Figure 13. Example of direct extraction of sand on Manoka Island in the Wouri estuary.

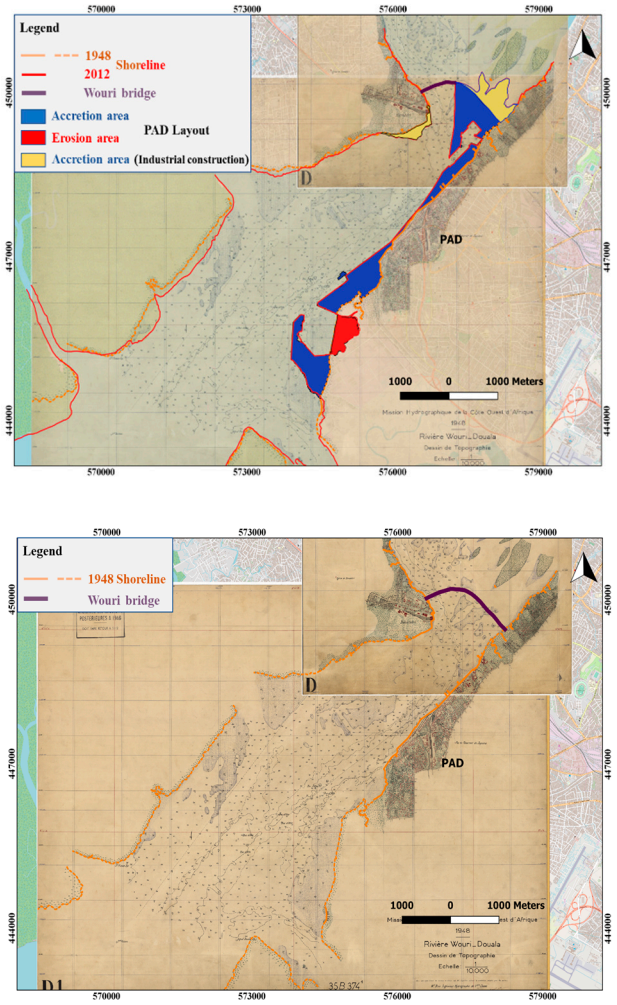

Figure 14. Geomorphological evolution of zone 5 by the construction of the Autonomous Port of Douala and industrial companies.

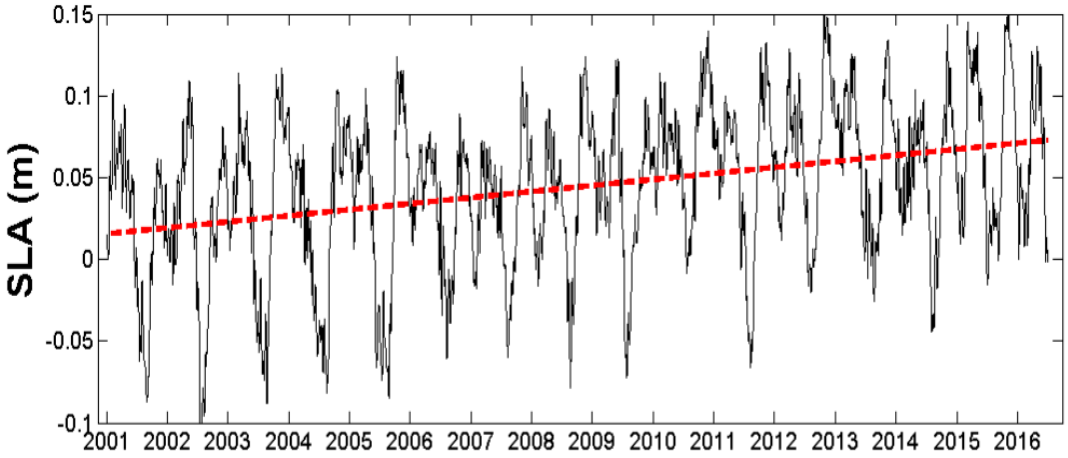

Figure 15. Evolution of mean spatial sea level anomaly (black) for the chosen grid nodes. The red line stands for trend (3.4 mm/year).

The Wouri estuary, by virtue of its configuration, is open in the southern section and undergoes lateral and frontal erosion of the coastline (natural erosion), due respectively to marine agitation as a result of external swells and wind flaps, and to migration from the mouth [39]. This may explain the variation of 379 ha in 64 years, due to erosion in zone 1 (Cape Cameroon). According to the authors

of [14], significant changes in the position of the coastline of the Wouri estuary were observed at the entrance to the estuary, namely the "Cape Cameroon" area, because it experienced a coastal retreat of more than 300 m for 30 years between 1986–2015. This dominance of variation by erosion in the area of the mouth has also been observed in other places in the world [40–49].

In addition, the dominance of variation by erosion can be explained by:

Sea level rise

Sea-level rise caused by climate change in the 21st century is exposing land previously inaccessible to waves and currents and is accompanied by severe coastal erosion that is slowly submerging the coasts of the Gulf of Guinea [50]. According to the authors of [4], the risk of coastal erosion in the Wouri estuary is reinforced by the trend of sea-level rise caused by global climate change and amplified by subsidence movement. The engulfing of the communication relay antenna installed in the continental part of Cape Cameroon (zone 1) (Figure 12) in 1992 marks the intensification of coastal erosion observed at the beginning of the 21st century. This suggests that Cape Cameroon (zone 1) is highly vulnerable to the increased erosion associated with rising water levels. This confirms the observations of the authors of [11], and the 2005 communication of the Ministry of Environment on the loss of land by flooding of about 4959 hectares, for a sea level rise of 20 cm, or 4.5% of the total area of mangroves [10]. If this increase continues, the consequences for the Wouri estuary coast would be enormous, because the rise in sea level due to global warming leads to an increase in mangrove losses from the Cameroonian coast (estimated at 300 ha per year) [51]. Very few studies have been conducted on the sensitivity of Cameroonian mangroves to climate change. One of the most recent is the pilot study on climate change impacts and adaptation measures on mangroves in the Wouri estuary [52]. This study used a combination of expert advice, the use of climate models and similar studies to assess the impacts of climate change on mangroves in the Wouri estuary. The floodplain is estimated at 49.5 km^2 for a sea level rise (SLR) of 0.20 m, and 330 km^2 for a SLR of 0.90 m, requiring the forced displacement of 57.8% of fishermen in the mangrove area. In the same vein, Ellison (2012) in her study of the vulnerability of mangroves in the Cameroonian estuary to climate change, estimated that the coastline has declined by about 3 m per year over the past three decades, and that an offshore mangrove island would have suffered 89% loss. So, at the coastal level, mangrove degradation may increase, coastal erosion will accelerate further and the risk of partial or total flooding will increase. The loss of land will then lead to the destruction of sandy beaches and consequently, localities such as Cape Cameroon and others will be at risk of disappearing.

Mangrove Harvesting and Sand Mining

Population growth in the Wouri estuary is associated with increased erosion because of destroying mangroves [7,9,11,14,38,53] and sand extraction activity [4,38]. This situation could be verified on the one hand by comparing two satellite images at different times. Indeed, by comparing the images of 2000 and 2014 (Figure 11), we can visualize a strong expansion of human installations in 2014 and the dynamics of land use on mangrove degradation. This observation shows the high population growth and the pressure on mangroves responsible for the evolution of geomorphological changes [9,11,27]. On the other hand, the extraction of sand in a disordered way is an observed daily occurrence (Figure 13). This sand extraction activity is carried out in the Wouri estuary, without distinction of areas, so that some sites are overexploited, reducing the volume of the beach, weakening the beach and thus increasing erosion. If nothing is done to coordinate these activities, the risks of erosion observed will continue to increase.

According to the authors of [39], the mouth center of the Wouri estuary functions as an open lagoon and is protected from the open sea by a unique sandy barrier, frequently cut by storm waves, but which is fairly resistant to erosion despite its narrow width. This shows the high sedimentation character encountered in the upstream section of this estuary [25,54]. In this study, this section showed, on the one hand, a strong accretion in zone 5 marked by embankments for the expansion of the PAD and the construction of industrial companies between 1948 and 1996 (212.66 ha) (zone 5) (Figure 14), accompanied by channel dredging works multiplying the turbulences of the environment

(resuspension) and promoting the significant accretion of 150.92 ha recorded in zone 4 between 1996 and 2012. This observation corroborates with the variations towards accretion upstream of Lobé Falls following the construction of the Kribi Port [14], and confirms the work of the authors of [25,55], who show that the access channel (upstream) to the PAD is highly silted and that the quantity of dredged sediments greatly exceeds the forecasts of previous studies [54]. This same scenario is observed in several port cities around the world [43,56,57].

Additionally, an inversion of the erosion variation trend for accretion was observed in zone 8, suggesting a rise in dredging waste dumped downstream of the estuary caused by the currents stopped at the tip of zone 8 (Souellaba).

The geospatial methods and automatic statistical calculation of the DSAS model, for the analysis of temporal spatial evolution variations in this study, proved to be very effective and advantageous. The estuarine coastline of Wouri Cameroon, represented by coastline features extracted from topographic minutes, nautical chart and spatial chart vectors, was studied by transects spaced 10 m apart generated by the DSAS model. According to the results obtained, this study provides local coastal managers and decision-makers with a reliable decision-making tool for the management of the Cameroonian coast.

6. Conclusions

The analysis of the evolutionary dynamics of the Wouri estuary (Cameroon) between 1948 and 2012 is of major interest for the qualification and quantification of evolutionary variations that have naturally and economically affected the estuarine environment. The observed morphological changes were calculated according to three periods: 1948–1996, 1996–2012 and 1948–2012, using geospatial methods and the automatic statistical calculation of the Digital Coastal Analysis System (DSAS). The results reveal an inhomogeneous evolution at the spatial and temporal scale. This is justified on one hand by an erosion dominance of 262.83 ha for −3.2 m/year and 110.56 ha for −5.8 m/year observed in zone 1 between 1948–1996 and 1996–2012 respectively, versus an accretion dominance of 239.17 ha for 4.3 m/year observed between 1948–1996 in zone 5 and 150.82 ha for 12.6 m/year between 1996–2012 in zone 4. On the other hand, a non-variation dominance of 17.27 ha in zone 7 and 30.8 ha in zone 8 between 1948–1996 and 1996–2012 was shown, respectively. Also, in zone 8, we observed an inversion of the trend of erosion variation between 1948 and 1996 for accretion between 1996 and 2012. This suggests that dredge discharges downstream of the estuary are rising.

After analysis, this study reveals the presence of amplifying factors (anthropogenic pressure and climate change) in the rate of change in morphological evolution at the beginning of the 21st century compared to the middle of the 20th century. An example is the photo-interpretation showing the high population growth and pressure on mangroves, the high rise of water in zone 1 (Cape Cameroon), sand mining and the backfilling in zone 5 (Douala) for the expansion of the PAD and the construction of industrial companies. Thus, the temporal spatial variations of the Wouri estuarine coast between 1948 and 2012 show a variation by erosion and accretion. According to the authors of [58], average erosion or accretion rates above ±2 m/year in zones can qualify them as zones highly vulnerable to erosion or accretion and should be confined as high risk zones. Therefore, significantly high rates and areas of erosion in zone 1 qualifies the area as being high-risk, and deserves the highest priority to mitigate the effects of erosion due to human activities observed at the beginning of the 21st century. Conversely, zones 4 and 5, with very high accretion rates and area, confirm the strong silting of the channel as shown by the authors of [25,55,59]

Author Contributions: Conceptualization, Y.F.F., N.P., I.B., R.O. and J.E.; Data curation, Y.F.F; Investigation, Y.F.F.; Methodology, Y.F.F., N.P., I.B., and R.O..; Resources, Y.F.F.; Software, Y.F.F.; Validation, N.P., I.B. and R.O.; Writing—original draft, Y.F.F.; Writing—review and editing, N.P., I.B. and R.O.

Funding: This PhD project was funded by the Service of the French Embassy in Cameroon (SCAC) through a fellowship to Y. FOSSI FOTSI. Hydrographic field sheets are stored at Shom's archives and used in this study, thanks to the hosting agreement with Shom University of Douala (n∘ 34/2017).

Acknowledgments: The authors would like to thank Yann Ferret, Alexa Latapy, Mathieu Bastien, Didier Bénéteau, Thierry Gendrier of Shom, Guillaume Marie, of University of Quebec at Romuski (UQAR) and the Service of the French Embassy in Cameroon (SCAC), the LIENSs laboratory (CNRS/La Rochelle University) and Shom (Brest), in accordance with the hosting agreement at Shom University of Douala—article 3, for their support in making this work.

Conflicts of Interest: The authors declare no conflict of interest

References

1. Luijendijk, A.; Hagenaars, G.; Ranasinghe, R.; Baart, F.; Donchyts, G.; Aarninkhof, S. The State of the World's Beaches. *Sci. Rep.* **2018**, *8*, 6641. [CrossRef] [PubMed]
2. Bird, E.C.F. *Coastline Changes. A Global Review*; Wiley: Chichester, UK, 1985.
3. Angoni, H.; Tatchim, A.P.; Nkonmeneck, B.A.; Nguekam, E. Utilisation du bois dans les pêcheries côtières du Cameroun. *Rev. D'ethnoécologie* **2015**. [CrossRef]
4. Ngangué, G.C.D. Enjeux de l'anthropisation d'un écosystème Humide Tropical et Impacts Environnementaux. Ph.D. Thesis, Université de Douala, Douala, Cameroun, 2013.
5. Sánchez-Arcilla, A.; García-León, M.; Garcia, V.; Devoy, R.; Stanica, A.; Gault, J. Managing coastal environments under climate change: Pathways to adaptation. *Sci. Total Environ.* **2016**, *572*, 1336–1352. [CrossRef] [PubMed]
6. Addo, K.A.; Larbi, L.; Amisigo, B.; Ofori-Danson, P.K. Impacts of Coastal Inundation Due to Climate Change in a CLUSTER of Urban Coastal Communities in Ghana, West Africa. *Remote Sens.* **2011**, *3*, 2029–2050. [CrossRef]
7. Magadza, C.H.D. Climate Change Impacts and Human Settlements in Africa: Prospects for Adaptation. *Environ. Monit. Assess.* **2000**, *61*, 193–205. [CrossRef]
8. Mainet, G. *Douala Croissance et Servitudes*; L'Harmattan: Paris, France, 1985.
9. Ellison, J.; Zouh, L. Vulnerability to Climate Change of Mangroves: Assessment from Cameroon, Central Africa. *Biology* **2012**, *1*, 617–638. [CrossRef] [PubMed]
10. Ngeunga, M. *Envahie Par Les Eaux, l'île de Cap Cameroun en Voie de Disparition*. 2015. Available online: https://www.lacite.info/voices2paris-1/2015/11/20/face-a-la-montde-disparition (accessed on 26 July 2019).
11. Mbevo Fendoung, P.; Tchindjang, M.; Fedoung, E.F. Analyse par télédétection de la vulnérabilité de la réserve de mangrove de Mabe face aux changements climatiques, entre 1986 et 2014. *Researchgate* **2017**, *65*. Available online: http://hdl.handle.net/2268/238117 (accessed on 26 July 2019).
12. Baro, J.; Mering, C.; Vachier, C. Peut-on cartographier des taches urbaines à partir d'images Google Earth. Une expérience réalisée à partir d'images de villes d'Afrique de l'Ouest. *Cybergeo Eur. J. Geogr.* **2014**. [CrossRef]
13. Ellison, J.C. Vulnerability assessment of mangroves to climate change and sea-level rise impacts. *Wetl. Ecol. Manag.* **2015**, *23*, 115–137. [CrossRef]
14. Ondoa, G.A.; Onguéné, R.; Eyango, M.T.; Duhaut, T.; Mama, C.; Angnuureng, D.B.; Almar, R. Assessment of the Evolution of Cameroon Coastline: An Overview from 1986 to 2015. *J. Coast. Res.* **2018**, *81*, 122–129. [CrossRef]
15. SMID. Appel Public à l'Epargne pour la Création de la société M"tropolitaire d'Investissement de Douala (SMID). Information Note. 2018. Available online: https://slideplayer.fr/slide/14913002/ (accessed on 26 July 2019).
16. Himmelstoss, E.A.; Henderson, R.E.; Kratzmann, M.G.; Farris, A.S. *Digital Shoreline Analysis System (DSAS) Version 5.0 User Guide*; USGS Numbered Series 2018–1179; U.S. Geological Survey: Reston, VA, USA, 2018.
17. Alemayehu, F.; Richard, O.; Kinyanjui, M.J.; Oliverv, W. Assessment of Shoreline Changes in the Period 1969–2010 in Watamuarea, Kenya. *Glob. J. Sci. Front. Res.* **2014**, *14*, 19–31.
18. Ayadi, K.; Boutiba, M.; Sabatier, F.; Guettouche, M.S. Detection and analysis of historical variations in the shoreline, using digital aerial photos, satellite images, and topographic surveys DGPS: case of the Bejaia bay (East Algeria). *Arab. J. Geosci.* **2016**, *9*, 26. [CrossRef]
19. Kermani, S.; Boutiba, M.; Guendouz, M.; Guettouche, M.S.; Khelfani, D. Detection and analysis of shoreline changes using geospatial tools and automatic computation: Case of jijelian sandy coast (East Algeria). *Ocean Coast. Manag.* **2016**, *132*, 46–58. [CrossRef]

20. Oyedotun, T.D.T. Shoreline Geometry: DSAS as a Tool for Historical Trend Analysis. *Geomorphol. Technol.* **2014**, *3*, 1–12.
21. Le Floch, J.F. Propagation de la Marée Dans l'Estuaire de la Seine et en Seine Maritime. Ph.D. Thesis, University of Paris, Paris, France, 1961.
22. Nichols, M.M.; Biggs, R.B. Estuaries. In *Coastal Sedimentary Environments*; Davis, R.A., Ed.; Springer: New York, NY, USA, 1985; pp. 77–186.
23. Ndongo, B.; Mbouendeu, S.L.; Tirmou, A.A.; Njila, R.N.; Dalle, J.D.M. Tendances pluviométriques et impact de la marée sur le drainage en zone d'estuaire: cas du Wouri au Cameroun. *Afr. Sci. Rev. Int. Sci. Technol.* **2015**, *11*, 173–182.
24. Morin, S.; Kuété, M. Le littoral Camerounais: problèmes morphologiques. *Trav. Lab. Géographie Phys. Appliquée* **1988**, *11*, 5–52. [CrossRef]
25. Fotsi, Y.F. *Etudes des Paramètres Hydrodynamiques de Contrôle de la Sédimentation Dans L'estuaire du Wouri au Cameroun*; University of douala: Douala, Cameroon, 2014.
26. Din, N.; Saenger, P.; Jules, P.R.; Siegfried, D.D.; Basco, F. Logging activities in mangrove forests: A case study of Douala Cameroon. *Afr. J. Environ. Sci. Technol.* **2008**, *2*, 22–30.
27. Ngo-Massou, V.M.; Essomè-Koum, G.L.; Kottè-Mapoko, E.; Din, N. Biology and Distribution of Mangrove Crabs in the Wouri River Estuary, Douala, Cameroon. *J. Water Resour. Prot.* **2014**, *6*, 236–248. [CrossRef]
28. Créach, R.; Bosch, S.; Boutry, L.; Genevier, J.; Claverie, P.; Badez, A. ScanBathy: A new solution to digitize depth data from historic survey sheets. In Proceedings of the 11th Annual GEBCO Bathymetric Science Day, Valparaiso, Chile, 12 October 2016.
29. Chapuis, O. L'École Polytechnique et les hydrographes de la Marine. Bull. Sabix Société Amis Bibl. *Hist. Lécole Polytech.* **2004**, *35*, 32–36.
30. Hamden, M.H.; Md Din, A.H. A review of advancement of hydrographic surveying towards ellipsoidal referenced surveying technique. *IOP Conf. Ser. Earth Environ. Sci.* **2018**, *169*, 012019. [CrossRef]
31. Shom, L. Shom C-7578-INT 2905-Approches de l'estuaire du Cameroun et de Malabo Librairie Maritime Nautic Way. 2008. Available online: https://www.nautic-way.com/fr_FR/carte-marine-shom-raster-ocean-atlantique/shom-raster-7578-int-2905-approches-de-l-estuaire-du-cameroun-et-de-malabo (accessed on 26 July 2019).
32. Trebossen, H. Apport Des Images RADAR à Synthèse d'Ouverture à la Cartographie Marine. Ph.D. Thesis, Université de Marne-la-Vallée, Marne-la-Vallée, France, 2002.
33. Shom, L. Elaboration de la Spatiocarte Topographique Numérique S201201300 de l'estuaire du Cameroun et de l'île de Bioko (Afrique). Brest, France. 2013. Available online: https://www.nautic-way.com/fr_FR/carte-marine-shom-raster-ocean-atlantique/shom-raster-7578-int-2905-approches-de-l-estuaire-du-cameroun-et-de-malabo (accessed on 26 July 2019).
34. Fletcher, C.; Rooney, J.; Barbee, M.; Lim, S.C.; Richmond, B. *Mapping Shoreline Change Using Digital Orthophotogrammetry on Maui*. No SPEC. HW, USA. 2003, pp. 106–124. Available online: https://www.jstor.org/stable/25736602 (accessed on 26 July 2019).
35. Saranathan, E.; Chandrasekaran, R.; Manickaraj, D.S.; Kannan, M. Shoreline Changes in Tharangampadi Village, Nagapattinam District, Tamil Nadu, India—A Case Study. *J. Indian Soc. Remote Sens.* **2011**, *39*, 107–115. [CrossRef]
36. Moussaid, J.; Fora, A.A.; Zourarah, B.; Maanan, M.; Maanan, M. Using automatic computation to analyze the rate of shoreline change on the Kenitra coast, Morocco. *Ocean Eng.* **2015**, *102*, 71–77. [CrossRef]
37. Nassar, K.; Mahmod, W.E.; Fath, H.; Masria, A.; Nadaoka, K.; Negm, A. Shoreline change detection using DSAS technique: Case of North Sinai coast, Egypt. *Mar. Georesources Geotechnol.* **2018**, *37*, 17. [CrossRef]
38. Tchindjang, M.; Steck, B.; Bopda, A. *Construire la ville portuaire de demain en Afrique Atlantique*. Afrique Atlantique; Douala, 2019; ISBN 978-2-37687-271-9. Available online: https://www.editions-ems.fr/livres/collections/afrique-atlantique/ouvrage/525-construire-la-ville-portuaire-de-demain-en-afrique-atlantique.html (accessed on 26 July 2019).
39. Baltzer, F.; Lafond, L.R. *Marais Maritimes Tropicaux*. 1971, p. 24. Available online: https://books.google.fr/books?id=-f4fAQAAIAAJ&hl=fr&source=gbs_book_other_versions_r&cad=4 (accessed on 26 July 2019).
40. Boyd, R.; Dalrymple, R.; Zaitlin, B.A. Classification of clastic coastal depositional environments. *Sediment. Geol.* **1992**, *80*, 139–150. [CrossRef]

41. Cencini, C. Processus physiques et activités humaines dans l'évolution du delta du Pô, Italie | Journal de la recherche côtière. *Coast. Res.* **1998**, *14*, 3.
42. Durand, P. Approche méthodologique pour l'analyse de l'évolution des littoraux sableux par photo-interprétation. Exemple des plages situées entre les embouchures de l'Aude et de l'Hérault (Languedoc, France). *Photo-Interprétation. Euro. J. App. Remote Sens.* **2002**, *38*, 3–20. Available online: https://hal-paris1.archives-ouvertes.fr/hal-00420049 (accessed on 26 July 2019).
43. Faye, I.B.N.; Hénaff, A.; Gourmelon, F.; Diaw, A.T. Évolution du trait de côte à Nouakchott (Mauritanie) de 1954 à 2005 par photo-interprétation. *Norois Environ. Aménage. Société* **2008**, 11–27. Available online: https://journals.openedition.org/norois/2146 (accessed on 26 July 2019). [CrossRef]
44. Zargouni, F.; Louati, M. Le littoral entre l'actuelle embouchure de l'oued Miliane et Soliman, Tunisie. Analyse de l'évolution du trait de côte par photo-interprétation et système d'information géographique. *OpenEdition* **2013**, *19*, 209–224.
45. Mouzouri, M.; Zoulikha, I. Abhatoo: Évolution et morpho-dynamique de la plaine côtière de Saïdia (littoral méditerranéen du Nord-Est du Maroc) durant la période 1958–2006. *Rabat* **2011**, *33*, 65–76.
46. Sabatier, F.; Suanez, S. Evolution of the Rhone Delta coast since the end of the 19th century. *Géomorphologie Relief Process. Environ.* **2003**, *9*, 283–300. [CrossRef]
47. Tastet, J.P. *Quelques Considérations Sur Les Classifications des Côtes. La Morphologie Côtière Ivoirienne. Annales de l'Université d'Abidjan—Série (Sciences)—Tome VIII, 2*. 1972. Available online: https://books.google.com.ph/books?id=EQ4_AQAAIAAJ&q=1972+Quelques+Consid%C3%A9rations+Sur+Les+Classifications+des+C%C3%B4tes.+La+Morphologie+C%C3%B4ti%C3%A8re+Ivoirienne&dq=1972+Quelques+Consid%C3%A9rations+Sur+Les+Classifications+des+C%C3%B4tes.+La+Morphologie+C%C3%B4ti%C3%A8re+Ivoirienne&hl=fr&sa=X&ved=0ahUKEwjYmKvW_ffkAhUH7WEKHbNlDGgQ6AEIQjAF (accessed on 26 July 2019).
48. Tastet, J.-P. Environnements sédimentaires et structuraux quaternaires du littoral du Golfe de Guinée (Cote d'Ivoire, Togo, Bénin). Ph.D. Thesis, University of Bordeaux I, Bordeaux, France, 1979.
49. Touré, B.; Kouamé, K.F.; Souleye, W.; Collet, C.; Affian, K.; Ozer, A.; Biémi, J.; Rudant, J.-P. L'influence des actions anthropiques dans l'évolution historique d'un littoral sableux à forte dérive sédimentaire: la baie de Port-Bouët (Abidjan, Ivory Coast). *Géomorphologie Relief Process. Environ.* **2012**, *18*, 369–382.
50. Addo, K.A.; Jayson-Quashigah, P.N.; Kufogbe, K.S. Quantitative Analysis of Shoreline Change Using Medium Resolution Satellite Imagery in Keta, Ghana. *Mar. Sci.* **2011**, *1*, 1–9. [CrossRef]
51. FAO. *Policy and Strategies for the Sustainable Management of Mangrove Swamp Ecosystems in Cameroon*; Projet TCP/CMR: Douala, Cameroon, 2006; p. 30. Available online: https://books.google.com.hk/books?id=MR3ivG5EKGIC&printsec=frontcover&dq=Cameroon&hl=fr&sa=X&ved=0ahUKEwjoivXdiPjkAhWEUN4KHYJoAlsQ6AEIODAC#v=onepage&q=Cameroon&f=false (accessed on 26 July 2019).
52. Youmbi, E.; Cerceau-Larrival, M.; Verhille, A.; Carbonnier-Jarreau, M. Morphologie et germination in vitro du pollen de Dacryodes edulis (Burseraceae): Détermination des facteurs contrôlant la germination. *Grana* **1998**, *37*, 87–92. [CrossRef]
53. Ngeve, M.N.; der Stocken, T.V.; Menemenlis, D.; Koedam, N.; Triest, L. Contrasting Effects of Historical Sea Level Rise and Contemporary Ocean Currents on Regional Gene Flow of Rhizophora racemosa in Eastern Atlantic Mangroves. *PLoS ONE* **2016**, *11*, e0150950. [CrossRef] [PubMed]
54. Sogreah. *Etude du Schéma Directeur d'assainissement de la Ville de Douala et Maitrise d'œuvre d'une Tranche Prioritaire de Travaux Rapport Définitif Des Phases 3 et 4*. N 2 35 0038/DLN/FRB/PGN; Douala, Cameroun. April 2006. Available online: https://www.google.com/url?sa=t&rct=j&q=&esrc=s&source=web&cd=1&ved=2ahUKEwjpx43lsvjkAhWHBIgKHUppDJUQFjAAegQIAhAC&url=https%3A%2F%2Ffsmtoolbox.com%2Fassets%2Fpdf%2FSchema_directeur_assainissement_Douala_2005.pdf&usg=AOvVaw220ybA2XsBscypFleiLn5x (accessed on 26 July 2019).
55. Djombe Seppo, D. *Contribution A la Connaissance de la Dynamique Sedimentaire du Chenal D'acces au Port de Douala*. Douala, Internship Report. 2011. Available online: https://books.google.com.hk/books?id=-vvSnNudkTUC&printsec=frontcover&dq=Internship+report+2011&hl=fr&sa=X&ved=0ahUKEwiBqorZifjkAhUWIIgKHbIrCdcQ6AEIKDAA#v=onepage&q&f=false (accessed on 26 July 2019).

56. Gatto, P.; Carbognin, L. The Lagoon of Venice: natural environmental trend and man-induced modification/La Lagune de Venise: l'évolution naturelle et les modifications humaines. *Hydrol. Sci. Bull.* **1981**, *26*, 379–391. [CrossRef]
57. UEMOA. *Etudes de Suivi du Trait de Côte et Schéma Directeur Littoral de l'Afrique de l'Ouest*. 2010. Available online: https://mappemonde-archive.mgm.fr/num32/articles/art11404.html (accessed on 26 July 2019).
58. Thieler, E.R.; Hammar-Klose, E.S. *National Assessment of Coastal Vulnerability to Sea-Level Rise*; Preliminary Results for the U.S. Gulf of Mexico Coast; USGS Numbered Series 2000-179; USUG: Liston, VA, USA, 2000.
59. UNEP. *Etat de Référence du Dispositif de Conservation Marine et Cotiere en Afrique Centrale*. Internship Report 2. June 2015. Available online: https://www.iucn.org\T1\guilsinglrightfiles\T1\guilsinglrightetat_de_reference_2015_-_amp_af_centrale_0 (accessed on 26 July 2019).